Available online at www.sciencedirect.com

ScienceDirect

Journal of Nutritional Biochemistry 126 (2024) 109589

Journal of Nutritional Biochemistry

RESEARCH PAPER

All-*trans* retinoic acid induces lipophagy through the activation of the AMPK-Beclin1 signaling pathway and reduces Rubicon expression in adipocytes

Yuki Mori[†], Masashi Masuda[†,*], Risa Yoshida-Shimizu, Saki Aoyagi, Yuichiro Adachi, Anh The Nguyen, Yusuke Maruyama, Yosuke Okumura, Yuki Kamei, Maiko Sakai, Kohta Ohnishi, Hirokazu Ohminami, Yutaka Taketani

Department of Clinical Nutrition and Food Management, Institute of Biomedical Sciences, Tokushima University Graduate School, Tokushima, Tokushima 770-8503, Japan

Received 16 October 2023; received in revised form 27 December 2023; accepted 22 January 2024

Abstract

Lipophagy is defined as a lipolysis pathway that degrades lipid droplet (LD) *via* autophagy. All-*trans* retinoic acid (atRA), a metabolite of vitamin A, stimulates lipolysis through hormone-sensitive lipase and β-oxidation. However, the regulation of lipolysis by atRA-induced autophagy in adipocytes remains unclear. In this study, we investigated the effect of atRA on autophagy in epididymal fat of mice and the molecular mechanisms of autophagy in 3T3-L1 adipocytes. Western blotting showed that atRA decreased the expression of p62, a cargo receptor for autophagic degradation, and increased the expression of the lipidated LC3B (LC3B-II), an autophagy marker, in epididymal fat. Next, we confirmed that atRA increased autophagic flux in differentiated 3T3-L1 cells using the GFP-LC3-RFP-LC3ΔG probe. Immunofluorescent staining revealed that the colocalization of LC3B with perilipin increased in differentiated 3T3-L1 cells treated with atRA. The knockdown of *Atg5*, an essential gene in autophagy induction, partly suppressed the atRA-induced release of non-esterified fatty acid (NEFA) from LDs in differentiated 3T3-L1 cells. atRA time-dependently elicited the phosphorylation of AMPK and Beclin1, autophagy-inducing factors, in mature 3T3-L1 adipocytes. Inversely, atRA decreased the protein expression of Rubicon, an autophagy repressor, in differentiated 3T3-L1 cells and epididymal fat. Interestingly, the expression of ALDH1A1, atRA-synthesizing enzymes, increased in epididymal fat with decreased protein expression of Rubicon in aged mice. These results suggest that atRA may partially induce lipolysis through lipophagy by activating the AMPK-Beclin1 signaling pathway in the adipocytes and increased atRA levels may contribute to decreased Rubicon expression in the epididymal fat of aged mice. (248/250 words)

Keywords: Atra; Autophagy; Lipolysis; Aged; ALDH1A1.

1. Introduction

Obesity has spread worldwide and has become among the most considerable global health problems in many countries [1]. It is often caused by an imbalance between energy intake and expenditure, so the disturbed endocrine functions of adipose tissue consisting of hypertrophic adipocytes are associated with an increased risk of type 2 diabetes, hypertension, stroke, and coronary artery disease [2,3]. Much research suggests various therapeutic targets, including enhanced lipolysis, reduced adipogenesis, and increasing thermogenesis, contribute to ameliorating adipocyte hypertrophy [4]. The anti-obesity effect of drugs and nutrients has been studied; phosphate, sulforaphane, and all-*trans* retinoic acid (atRA) induce lipolysis in adipocytes [5–8].

Lipolysis is a catabolic process that plays an important role in triglyceride (TG) turnover. In this mechanism, adipose triglyceride lipase (ATGL), hormone-sensitive lipase (HSL), and monoglyceride lipase are the principal enzymes [9,10]. Unlike this canonical lipolysis, a recent study provides a new lipolysis pathway, termed lipophagy, in which lipid droplet (LD) is degraded *via* autophagy [11]. Autophagy is a highly conserved intracellular degradation system that a double-membrane structure called isolation membrane that engulfs cytoplasmic components, forming a vesicle (autophagosome), and their sequestered materials are decomposed by fusion with the lysosome [12,13]. Autophagy maintains cellular homeostasis by targeting proteins, RNA, LD, and damaged organelles [14,15]. During autophagy, LC3B is conjugated to the phosphatidylethanolamine (PE) molecule on the isolation membrane as lipidated LC3B (LC3B-II), an autophagy substrate, by the ATG12-ATG5-ATG16L1 complex after cleavage of glycine

* Corresponding author at: Department of Clinical Nutrition and Food Management, Institute of Biomedical Sciences, Tokushima University Graduate School, 3-18-15, Kuramoto-cho, Tokushima 770-8503, Japan. Tel.: +81-88-633-7093.
E-mail address: masuda.masashi@tokushima-u.ac.jp (M. Masuda).
† Contributed equally to this work.

https://doi.org/10.1016/j.jnutbio.2024.109589

120 residues of LC3B by ATG4, and LC3B-II contributes to the formation of the isolation membrane [12−14]. The activation of AMP-activated protein kinase (AMPK) or the inhibition of the mammalian target of rapamycin complex 1 (mTORC1) stimulates the driver of the isolation membrane formation such as unc-51 like autophagy activating kinase 1 (ULK1) [16,17]. Furthermore, the phosphorylation of AMPKα can induce phosphorylation of Beclin1, which regulates the isolation membrane formation and autophagosome-lysosome fusion, leading to upregulating autophagic flux [18]. On the other hand, Rubicon, an autophagy repressor, inhibits autophagosome-lysosome fusion by binding to the class III phosphatidylinositol-3 kinase (PI3K) complex [19]. While recent studies revealed that Rubicon mRNA and protein levels increase in some aged tissues, such as the kidney and liver, Rubicon expression decreases in aged adipose tissue [20,21]. Interestingly, age-dependent loss of Rubicon in adipose tissue causes systemic fat loss [21]. atRA, a metabolite of vitamin A (retinol), has important biological roles in reproduction, immune response, and development [22–24]. All-*trans* retinol is first converted to all-*trans* retinal and then irreversibly oxidized by the aldehyde dehydrogenase 1A (ALDH1A) family to form atRA [25]. Then, atRA is catalyzed to 4-OH-atRA by the cytochrome P450 family 26 (CYP26). Human studies have shown a negative correlation between serum retinol concentration and BMI, and a negative correlation between serum RA concentration and BMI and abdominal circumference [26,27]. The molecular mechanism by which atRA regulates a transcription for target genes mediated by specific nuclear receptors, including retinoic acid receptors (RARs), retinoid X receptors (RXRs), and the peroxisome proliferator-activated receptor (PPAR) β/δ [28,29]. atRA increases the phosphorylation of AMPKα and induces autophagy in acute promyelocytic leukemia (APL) cells [30]. Although it is suggested that atRA induces lipolysis by a PPARβ/δ-mediated increase in the level of HSL [8], whether atRA regulates lipolysis *via* autophagy in adipocytes has not yet been investigated.

In the present study, we evaluated the effect of atRA on autophagy in white adipose tissue (WAT) of mice and differentiated 3T3-L1 adipocytes. Furthermore, we also explored the molecular mechanism underlying the atRA-induced autophagic process in 3T3-L1 adipocytes.

2. Materials and methods

2.1. Chemicals and reagents

DMSO, atRA, mouse anti-β-actin monoclonal Ab (A5441), DMEM, FBS, insulin, dexamethasone, 3-isobutyl-1-methylxanthine, troglitazone, and Mission siRNA were purchased from Sigma-Aldrich (St. Louis, MO, USA). Buprenorphine hydrochloride was purchased from Otsuka Pharmaceutical Co., Ltd. (Tokyo, Japan). Pentobarbital sodium salt was purchased from Tokyo Kasei Co., Ltd. (Tokyo, Japan). RIPA buffer, anti-LC3B (#2775), anti-p62 (#5114), anti-Perilipin-1 (#9349), anti-ULK1 (#8054), anti-phospho-ULK1 (#5869, Ser555), anti-Beclin1 (#3495), anti-Rubicon (#8465), anti-AMPKα (#5831), anti-phospho-AMPKα (#50081, Thr172), anti-SCD1 (#2794) Ab were purchased from Cell Signaling Technology (Beverly, MA, USA). Anti-MAP LC3β (sc-271625), anti-ALDH1A1 (sc-374149), anti-phospho-EGFR (sc-57545, Tyr 1173), and anti-EGFR (sc-373746) Ab were purchased from Santa Cruz Biotechnology (Santa Cruz, CA, USA). Anti-ALDH1A2 (13951-1-AP), and anti-Adiponectin (21613-1-AP) were purchased from Proteintech (Rosemont, IL, USA). Phosphorylated Beclin-1 (#13232, Ser90/93/96) Ab was purchased from Signalway Antibody (College Park, MD, USA). Goat anti-rabbit IgG(H+L)-HRP conjugate (#1706515) was purchased from Bio-Rad (Hercules, CA, USA). Goat anti-mouse IgG(H+L)-HRP conjugate (#62-6520), Alexa Fluor 488, and Alexa Fluor 546 were purchased from Invitrogen (Carlsbad, CA, USA). Aqua-Poly/Mount (18606-20) is purchased from Polysciences, Inc (Warrington, PA, USA). OCT compound was purchased from Sakura FineTek (Tokyo, Japan). Penicillin-streptomycin, FFA-free BSA, and Chemi-Lumi One Super were purchased from Nacalai Tesque (Kyoto, Japan). Torin 1 (10997) was purchased from Cayman Chemical Co. (Ann Arbor, MI, USA). FuGENE HD Transfection Reagent was purchased from Promega Corporation (Madison, WI, USA). FluoroBrite DMEM (A1896701), Lipofectamine RNAiMAX transfection reagent, TRIzol Reagent, oligo(dT) primer, and SYBR Green master mix were purchased from Thermo Fisher Scientific (Waltham, MA, USA). M-MLV reverse transcriptase was purchased from Nippon Gene (Tokyo, Japan).

2.2. Animal experiments

The animal work took place in Division for Animal Researches and Genetic Engineering Support Center for Advanced Medical Sciences, Institute of Biomedical Sciences, Tokushima University Graduate School. The animals were housed in pathogen-free conditions and maintained under a standard 12 h light-dark cycle with free access to water. First, 35-week-old male C57BL/6J mice (Japan SLC, Shizuoka, Japan) were randomly divided into two groups (n=4 per group) and intraperitoneally administrated a total of 10 mg/kg body weight (BW) of atRA or 0.1% DMSO prepared in 500 μl sterile saline once every two days for 4 weeks. Each group of mice was fasted for 20 h with water ad libitum before sacrifice with a total of 0.1 mg/kg BW of buprenorphine hydrochloride and a total of 50 mg/kg BW of pentobarbital sodium salt. Secondly, 8-week-old male C57BL/6J mice (Japan SLC, Shizuoka, Japan) were randomly divided into two groups (n=4 per group) and a total of 10 mg/kg BW of atRA or 0.1% DMSO prepared in sterile saline was intraperitoneally administered, then the mice were euthanized 24 h later. Third, 8-week-old male and 100-week-old male C57BL/6J mice (Japan SLC, Shizuoka, Japan) were divided into two groups (n=5 per group). Each group of mice was fed ad libitum before they were euthanized. Epididymal fat samples were washed in 0.9% NaCl and immediately snap-frozen in liquid nitrogen and stored at −80 °C. These studies were approved by the Animal Experimentation Committee of Tokushima University School of Medicine (animal ethical clearance No. T28-88 and T30-66) and were carried out in accordance with guidelines for the Animal Care and Use Committee of Tokushima University School of Medicine.

2.3. Plasma parameters

Plasma triglyceride (TG) and non-esterified fatty acid (NEFA) levels were determined using commercial kit LabAssay Triglyceride (Wako, Osaka, Japan) and LabAssay NEFA (Wako) according to the manufacturer's instruction, respectively [5]. Absorbance was measured by SpectraMax ABS (Molecular Devices, Sunnyvale, CA, USA).

2.4. Histological assessments

Epididymal adipose tissues were fixed in 4% PFA/PBS at 4°C overnight, and then dehydrated in 30% sucrose/PBS at 4°C overnight. The tissues were embedded in OCT compound diluted with 30% sucrose/PBS. Tissues were cryo-sectioned at 10 μm thickness and the slides were stained with H&E according to a standard protocol. Adipocyte size was visualized using a BZ-9000 fluorescence microscope (Keyence, Osaka, Japan). Adipocyte area was quantified using the ImageJ imaging software program (NIH, Bethesda, MD, USA).

2.5. Western blot analysis

Tissue and cell lysates were prepared using RIPA buffer. Protein samples were heated at 95°C for 5 min in sample buffer in the presence of 5% 2-mercaptoethanol and subjected to SDS-PAGE. The separated proteins were transferred by electrophoresis to polyvinylidene difluoride transfer membranes (Immobilon-P, Millipore, MA, USA). The membranes were treated with diluted affinity-purified anti-LC3B (1:2000), anti-p62 (1:2000), anti-ULK1 (1:3000), anti-phospho-ULK1 (1:1500), anti-Beclin1(1:1500), anti-phospho-Beclin1 (1:1000), anti-Rubicon (1:2000), anti-ALDH1A1 (1:1000), anti-ALDH1A2 (1:1000), anti-AMPKα (1:2000), anti-phospho-AMPKα (1:3000) Ab, and anti-Adiponectin (1:2000). Mouse anti-β-actin monoclonal Ab was used as an internal control. Goat anti-rabbit IgG(H+L)-HRP conjugate or goat anti-mouse IgG(H+L)-HRP conjugate were utilized as a secondary Ab, and signals were detected using Chemi-Lumi One Super.

2.6. Quantitative PCR analysis

Total RNA was isolated from differentiated 3T3-L1 cells or epididymal adipose tissues using TRIzol Reagent according to the manufacture's instruction. Quantitative real-time PCR assays were performed by using an Applied Biosystems StepOne qPCR instrument. In brief, the cDNA was synthesized from 1 μg of total RNA using M-MLV reverse transcriptase with an oligo(dT) primer. After cDNA synthesis, quantitative real-time PCR was performed in 5 μl of Fast SYBR Green master mix. The primer sequences are as follows: mouse *Rubicon* (5'-CTCATCCATGACCAGGTGTG-3' and 5'-GTCGCTCATGCAAACTGA-3'), mouse *Aldh1a1* (5'-ATACTTGTCGGATTTAGGAGGCT-3' and 5'-GGGCCTATCTTCCAAATGAACA-3'), mouse *Glut1* (5'-CATCGTGGCCA TCTTTGGCTTTGT-3' and 5'-GGAAGCACATGCCCACAATGAAGT-3'), mouse *Orp8* (5'-GCCTTAGCAGACGGAGAACC-3' and 5'-GCTACAACAG TTGATGGCCC-3'), and mouse *β-actin* (5'-CTGACCCTGAAGTACCCC ATTGAACA-3' and 5'-CTGGGGTGTTGAAGGTCTCAAACATG-3'). The quantification of given genes was expressed as the mRNA levels normalized to a ribosomal housekeeping gene *β-actin* using the $\Delta\Delta$Ct method.

2.7. Cell culture and establishment of stable cell lines

Mouse fibroblast line 3T3-L1 pre-adipocytes (JCRB9014) were obtained from the Health Science Research Resources Bank (Osaka, Japan). The 3T3-L1 pre-adipocytes were cultured as described previously [6]. Briefly, 3T3-L1 pre-adipocytes were maintained in high-glucose DMEM containing 10% FBS and 1% penicillin streptomycin at 37°C in an atmosphere containing 5% CO_2. To induce the differentiation of the pre-adipocytes into mature adipocytes, 100% confluent cells were maintained for 2 days and changed to differentiation medium (DMEM containing 10% FBS, 10 μg/ml insulin, 1 μM dexamethasone, 500 μM 3-isobutyl-1-methylxanthine, and 1 μM troglitazone). Two days later, the media were replaced with DMEM containing 10% FBS and refreshed every other day for an additional 6–10 days. Retroviral plasmid vector of pMRX-IP-GFP-LC3-RFP-LC3ΔG (RDB14600) developed by Dr. Noboru Mizushima was obtained from RIKEN BRC DNA BANK (Tsukuba, Japan) [31]. Stable 3T3-L1 cells expressing GFP-LC3-RFP-LC3ΔG were generated as we previously described [7].

2.8. RNAi experiments

Differentiated 3T3-L1 cells were transfected with siRNA directed against *Atg5* (SASI_Mm01_00089196 and SASI_Mm01_00089197; Sigma-Aldrich) [7], *AMPKα1/2* (sc-45313; Santa Cruz Biotechnology) [7], *Aldh1a1* (SASI_Mm01_00044509; Sigma-Aldrich), or negative control (SIC001; Sigma-Aldrich) using Lipofectamine RNAiMAX transfection reagent, according to the manufacturer's instruction. The expression levels were assessed after 48 h using real-time PCR.

2.9. Detection of NEFA in medium

NEFA content in medium was determined as described previously [7]. To determine the release of fatty acids from LD in differentiated 3T3-L1 cells, detection of NEFA in the medium was performed using 48-well tissue culture plates. Cells were differentiated into mature adipocytes and transfection with 100 pmol *Atg5* siRNA, 100 pmol *AMPKα1/2* siRNA, or control for 24−48 h, followed by replacement 2% FFA-free BSA culture medium and the treatment with vehicle (DMSO), 100 nM atRA, or 250 nM Torin 1 for 24 h. After collecting the medium, NEFA content in the conditioned medium was measured with a commercial kit LabAssay NEFA (Wako) according to the manufacture's protocol.

2.10. Autophagic flux assay

For GFP-LC3-RFP-LC3ΔG microplate assay was performed as described previously [7]. Wild-type (as background) or stable 3T3-L1 cells expressing GFP-LC3-RFP-LC3ΔG were seeded into 96-well plates (Greiner CELLSTAR #655090, Greiner Bio-One, Germany). After the differentiation of the pre-adipocytes into mature adipocytes, they were treated with vehicle (DMSO), 100 nM atRA, or 250 nM Torin 1 as positive control for 12 h. Following washing with FluoroBrite DMEM twice, cells were imaged by using Operetta high-content imaging system (PerkinElmer, MA, USA) at 40x magnification at following settings: for EGFP (λ ex: 460−490 nm, λ ex: 500−550 nm) and for RFP (λ ex: 530−560 nm, λ ex: 570−650 nm).

2.11. Immunofluorescent staining

Differentiated 3T3-L1 cells were washed two times in PBS, and fixed in cold 3% PFA/PBS at room temperature (RT) for 15 min. After washing with PBS, Heat-induced epitope retrieval was performed with the citric acid (ph=6.0) for 10 min, followed by washing three times with PBS. Differentiated 3T3-L1 cells were processed by 0.1% Triton X-100/PBS at 4°C for 10 min, followed by washing three times with PBS. Blocking was performed with 1% BSA/ PBS containing 0.1% Tween-20 at RT for 30 min, followed by washing three times with PBS. Perilipin-1 (1:200), and MAP LC3β (1:200) were applied at 4°C overnight to cells. After washing with PBS, cells were incubated at RT for 1 h with secondary antibodies prepared at 1:200 in Ab dilution buffer: Alexa Fluor 488 and Alexa Fluor 548. After the secondary antibodies were removed and cells were washed with PBS, cells were mounted in Aqua Poly/Mount. Fluorescence was visualized using a Nikon A1R confocal microscope (Nikon, Tokyo, Japan). Quantification of data was performed using the ImageJ imaging software program (NIH, Bethesda, MD, USA).

2.12. Oil red-O staining

To determine the lipid accumulated in differentiated 3T3-L1 cells, oil red-O staining was performed using 48-well tissue culture plates. Cells were differentiated into mature adipocytes and transfection with 100 pmol *Atg5* siRNA or control for 48 h, then the treatment with DMSO or 100 nM atRA for 10 d. After removing the medium and washing twice with PBS, the cells were fixed with 3% PFA/PBS for 10 min. After washing with PBS, 60% isopropanol was

added for 1 min and stained with oil red-O diluted with 60% isopropanol for 20 min. After rinsing with 60% isopropanol and PBS, the cells were photographed under a BZ-9000 fluorescence microscope. Lipid accumulation was quantified using the ImageJ imaging software program.

2.13. Statistical analysis

Data were collected from more than two independent experiments and were reported as the means±S.E.M. Statistical analysis for two-group comparison was performed using a two-tailed Student's *t* test, or one-way ANOVA with a Student-Newman post-hoc test for multi-group comparison. All data analysis was performed using GraphPad Prism 5 software (Graphpad Software, San Diego, CA, USA). $P<.05$ was considered statistically significant.

3. Results

3.1. atRA reduces the size of adipocytes and increases the LC3B-II expression in the epididymal fat of mice

First, we investigated the effect of atRA on autophagy in adipose tissue of mice intraperitoneally treated with DMSO (Control) or atRA for 4 weeks. The plasma TG and NEFA concentrations showed no significant difference between the control and atRA groups (Table 1). The body weight was lower by about 10% in the atRA group than in the control group. In the atRA group, tissue weight adjusted by BW of the epididymal fat significantly decreased (Fig. 1A). However, atRA tended to decrease tissue weight of retroperitoneal fat and subcutaneous fat and did not affect that of brown adipose tissue weight. In addition, HE staining showed that epididymal adipocyte area decreased in the atRA group (Fig. 1B). We next investigated whether atRA affects autophagy-related protein expression in the epididymal fat. Western blotting revealed that atRA decreased the protein expression of p62, a cargo receptor for autophagic degradation, and increased the LC3B-II protein expression in the epididymal fat (Fig. 1C and D). Recent research suggests that oxysterol-binding protein-related protein 8 (ORP8), which is located on LDs and mediates the encapsulation of LDs by autophagosomal membranes, is a lipophagy receptor that plays a crucial role in cellular lipid metabolism [32]. Therefore, we evaluated the effect of atRA on the gene expression of *Orp8*. As

Table 1
Effects of atRA on plasma TG and NEFA levels

	Control	atRA
TG (mg/dl)	36.86±4.94	71.26±13.4
NEFA (mEq/dl)	0.46±0.04	0.57±0.06

Values are mean±S.E.M. (n=4/group). (Data was analyzed by two-tailed unpaired Student's *t* test).

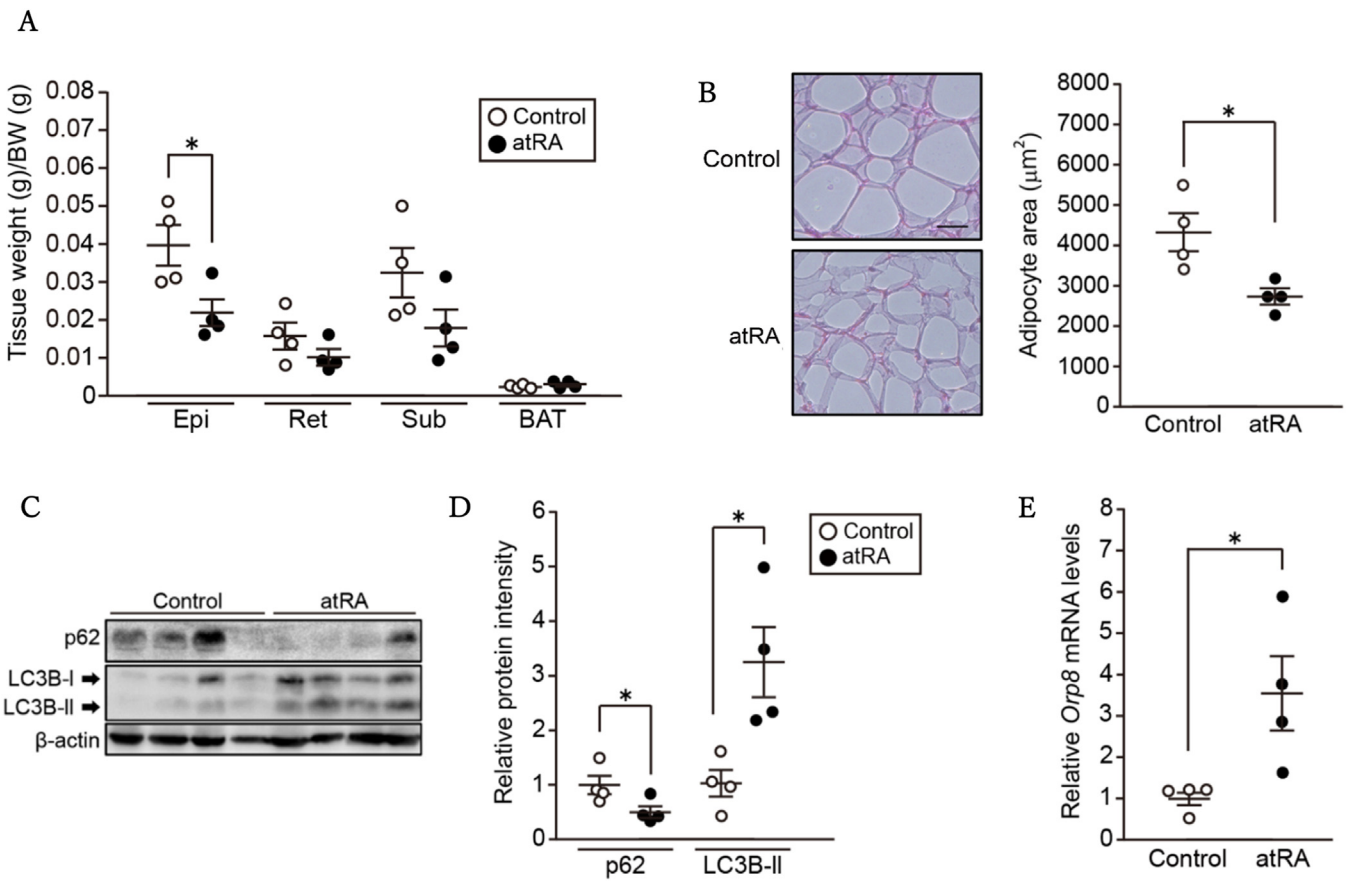

Fig. 1. Effects of atRA on the expression of autophagy-related proteins in the epididymal fat of mice. Thirty-five-week-old male C57BL/6J mice were treated with 0.1% DMSO (Control) or atRA (10 mg/kg) for 4 weeks. (A) Tissue weights of the epididymal fat (Epi), retroperitoneal fat (Ret), subcutaneous fat (Sub), and brown adipose tissue (BAT) were adjusted by body weight (BW). (B) Adipocytes from epididymal fat were stained with H&E for the determination of adipocyte size. Images were taken by microscope. Scale bar = 50 μm. Adipocyte area was calculated based on at least 100 adipocytes per group and was determined using ImageJ software. (C, D) Western blotting of LC3B and p62 in the epididymal fat. (E) Eight-week-old male C57BL/6J mice were treated with 0.1% DMSO (Control) or atRA (10 mg/kg) for 24 h. The *Orp8* mRNA was detected by real-time PCR in epididymal fat. *β-actin* was used as an internal control. Values are mean±S.E.M. (n=4). $^*P<.05$ (two-tailed unpaired Student's *t* test).

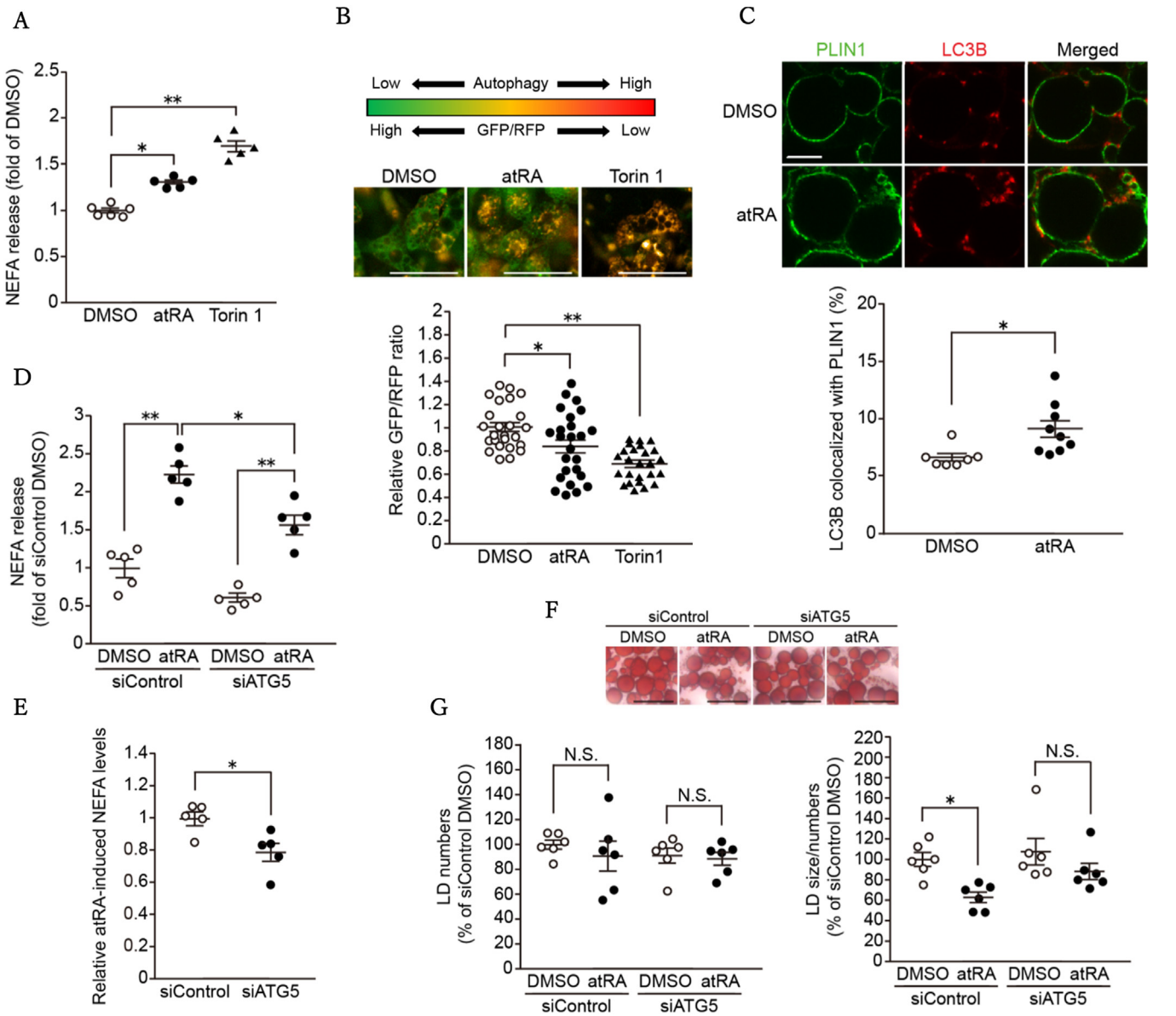

Fig. 2. Effect of atRA on the lipolysis of LD through autophagy in 3T3-L1 adipocytes. (A) Differentiated 3T3-L1 cells were treated with 100 nM atRA, 250 nM Torin 1, or 0.1% DMSO (Control) in DMEM containing 2% BSA-FFA for 24 h (n=5–6). The culture medium was collected and assayed for NEFA content (mEq/L/mg protein). (B) Autophagic flux in differentiated 3T3-L1 cells stably expressing GFP-LC3-RFP-LC3ΔG treated with atRA, Torin 1, or DMSO (Control) for 12 h (n=25). GFP/RFP ratio data were expressed as the fold-value against DMSO. Scale bar = 50 μm. $^{*}P$<.05, $^{**}P$<.01 (one-way ANOVA with a Student-Newman *post-hoc* test). (C) After differentiated 3T3-L1 adipocytes were treated with atRA or DMSO (Control) for 12 h (n=7–9), cells were fixed and stained for PLIN1 Ab conjugated to Alexa Fluor 488 (green) and LC3B Ab conjugated to Alexa Fluor 546 (red). Images were taken with a confocal laser-scanning microscope. Percentage colocalization of LC3B with PLIN1 was quantified using the ImageJ imaging software program. Scale bar = 10 μm. $^{*}P$<.05 (two-tailed unpaired Student's t test). (D, E) Differentiated 3T3-L1 adipocytes were treated with atRA or DMSO (Control) in DMEM containing 2% BSA-FFA for 24 h after transfection with 100 pmol *Atg5* siRNA (siATG5) or negative control (siControl) (n=5). The culture medium was collected and assayed for NEFA content (mEq/L/mg protein). $^{*}P$<.05, $^{**}P$<.01 (one-way ANOVA with a Student-Newman *post-hoc* test). The comparison of atRA-induced NEFA content (mEq/L/mg protein). $^{*}P$<.05 (two-tailed unpaired Student's t test). (F, G) Differentiated 3T3-L1 cells were treated with atRA or DMSO (Control) for 10 d after transfection with siATG5 or siControl (n=6). Cells were then fixed, stained with oil red-O staining, and analyzed with a BZ-9000 fluorescence microscope. LD size and numbers were quantified using the ImageJ imaging software program. Scale bar = 50 μm. $^{*}P$<.05, $^{**}P$<.01 (one-way ANOVA with a Student-Newman *post-hoc* test). NS, not significant.

a result, atRA increased *Orp8* mRNA expression in the epididymal adipose tissue of mice (Fig. 1E).

3.2. atRA partially contributes to lipolysis through autophagy in 3T3-L1 adipocytes

To clarify the involvement of autophagy in atRA-induced lipolysis, we analyzed the release of NEFA from LDs in differentiated 3T3-L1 cells. The NEFA levels in the media increased by either treatment of atRA or Torin 1, autophagy inducer (Fig. 2A). We next investigated whether atRA induces autophagic flux in mature 3T3-L1 cells by using an autophagic flux assay probe, the GFP-LC3-RFP-LC3ΔG [31]. The probe is cleaved by Atg4 under autophagy induction and divided into GFP-LC3 and RFP-LC3ΔG. After autophagosome-lysosome fusion, the interior GFP-LC3 is degraded, and the acidic environment of the autolysosome diminishes GFP fluorescence. However, RFP-LC3ΔG cannot be degraded because it is not incorporated into autophagosomes, so RFP fluorescence can be used as internal control due to its stability. Therefore, a decline in the GFP/RFP ratio indicates enhanced autophagy. We have

previously reported that sulforaphane decreased the GFP/RFP ratio in differentiated 3T3-L1 cells stably expressing the GFP-LC3-RFP-LC3ΔG [7]. In adipocytes stably expressing the GFP-LC3-RFP-LC3ΔG, treatment with atRA or Torin 1 significantly caused the reduction of the GFP/RFP ratio compared with DMSO (Fig. 2B). These results indicate that atRA increases autophagic flux in 3T3-L1 adipocytes. LDs are coated with various proteins that regulate lipid metabolism, such as the storage of TG and lipolysis in the LDs. Perilipins family proteins (PLIN1–5) are the most representative LD-associated proteins. In adipocytes, PLIN1 is the most abundant protein coating LDs [33,34]. Therefore, we examined the effects of atRA on the colocalization of LC3B with PLIN1 in adipocytes using immunofluorescent staining. The ratio of LC3B colocalized with PLIN1 increased by atRA in differentiated 3T3-L1 cells (Fig. 2C). In addition, we confirmed the effect of atRA on the gene expression of *Orp8*. Like *in vivo*, atRA increased *Orp8* mRNA expression in 3T3-L1 adipocytes (Supplementary Fig. S1A).

ATG5 is located downstream of the AMPK signaling pathway, which is one of the most famous autophagy induction pathways [12,16]. Therefore, to reveal the effect of atRA-induced autophagy on lipid accumulation, we used mature 3T3-L1 cells with knockdown of *Atg5* induced by *Atg5*-specific siRNA, as described previously [7]. We investigated the rapid effect of atRA for 24 h on the release of NEFA from LDs in 3T3-L1 adipocytes treated with *Atg5*-specific siRNA. *Atg5* knockdown partially suppressed the atRA-induced increase of the NEFA release from LDs in differentiated 3T3-L1 cells (Fig. 2D and E). In addition, *Atg5*-knockdown 3T3-L1 adipocytes and control 3T3-L1 adipocytes were treated with atRA or DMSO for 10 days, and then oil red-O staining was performed. No differences showed in the number of LDs in 3T3-L1 adipocytes between atRA treatment and DMSO. *Atg5* knockdown inhibited the atRA-induced reduction in the LD size in 3T3-L1 adipocytes (Fig. 2F and G). These results indicate that atRA partially induces lipolysis through autophagy in 3T3-L1 adipocytes.

3.3. atRA induces the activation of AMPK-Beclin1 signaling pathway and decreases Rubicon in 3T3-L1 adipocytes and the epididymal fat of mice

The phosphorylation of ULK1 and Beclin1 by activated AMPKα is one of the most popular mechanisms of autophagy induction [16–18]. Previous report showed that atRA induces AMPKα activation in APL cells [30]. To investigate the molecular mechanisms by which atRA induces autophagy in 3T3-L1 adipocytes, we monitored the time-dependent effects of atRA on the phosphorylation of AMPKα, ULK1, and Beclin1. Western blotting showed that phosphorylated-AMPKα (p-AMPKα) levels significantly increased after 9, 10, and 12 h of atRA treatment (Fig. 3A and B). Furthermore, atRA significantly increased phosphorylated-Beclin1 (p-Beclin1) levels for 8, 9, and 12 h compared with DMSO. However, phosphorylated-ULK1 (p-ULK1) levels showed no significant difference in atRA compared with DMSO at each time up to 12 h. Recently, it was reported that reducing Rubicon, a protein that inhibits autophagy, increases autophagic flux in white adipose tissues and adipocytes of mice [21]. To clarify whether atRA affects the Rubicon expression, we evaluated the time-dependent effects of atRA on Rubicon protein expression in 3T3-L1 adipocytes. Expectedly, atRA treatment significantly reduced Rubicon protein levels at 10 h in differentiated 3T3-L1 cells (Fig. 3C and D). However, *Rubicon* mRNA expression was not changed after atRA treatment up to 10 h (Fig. 3E). The activation of the AMPK-Beclin1 signaling pathway and the reduction of Rubicon are the mechanisms of autophagy induction. However, we reported that AMPK is involved in lipophagy in adipocytes [7], but it has been reported that the reduction of Rubicon does not induce lipolysis in mouse adipocytes [21]. Therefore, to clarify whether atRA induces lipolysis *via* the AMPK-Beclin1 signaling pathway in adipocytes, we used mature 3T3-L1 cells with knockdown of *AMPKα1/2* induced by *AMPKα1/2*-specific siRNA as described previously [7]. *AMPKα1/2* knockdown suppressed the atRA-induced release of NEFA from LD in differentiated 3T3-L1 cells by about 30% (Fig. 3F and G). These results suggest that atRA induces lipophagy by activating the AMPK-Beclin1 signaling pathway in 3T3-L1 adipocytes.

Table 2
Effects of atRA on plasma TG and NEFA levels

	Control	atRA
TG (mg/dl)	52.85±1.80	72.0±15.3
NEFA (mEq/dl)	0.38±0.03	0.46±0.04

Values are mean±S.E.M. (n=4/group). (Data was analyzed by two-tailed unpaired Student's t test).

Next, mice were treated with atRA at 10 mg/kg body weight for 24 h to confirm the regulation of p-AMPK, p-Beclin1, and Rubicon expression by atRA *in vivo*. Plasma TG and NEFA levels showed no significant difference between the control and atRA groups (Table 2). Similarly to *in vitro* results, atRA treatment induced an increase in the phosphorylation of AMPK, a little increase in the phosphorylation of Beclin1, and a decrease in the Rubicon protein expression in the epididymal fat of mice compared with the control (Fig. 4A–D). The p62 and the LC3B-II protein expression tended to decrease in the atRA-treated group. However, the expression of *Rubicon* mRNA was unchanged in the epididymal fat of mice treated with atRA (Fig. 4E). These results suggest that atRA may accelerate autophagy by activating the AMPK-Beclin1 signaling pathway and decreasing Rubicon protein expression in the epididymal fat, just like *in vitro*.

3.4. Aging increases ALDH1A1 expression in the epididymal fat of mice

Rubicon protein expression in the epididymal fat of aged mice is lower than in young mice [21]. However, the direct cause of the decrease in Rubicon protein in the adipose tissue of aged mice remains unknown. We hypothesized that atRA levels in the epididymal fat of aged mice are higher than that of young mice, decreasing Rubicon expression. To clarify the relationship between the reduction of Rubicon and atRA levels in the adipose tissue of aged mice, we first examined Rubicon expression in the epididymal fat of 100-week-old mice. We confirmed that the Rubicon and p62 protein in the epididymal fat of aged mice were lower than that of young mice (Fig. 5A and B). In addition, qPCR showed that *Rubicon* mRNA expression tended to decrease in the epididymal fat of aged mice (Fig. 5C). Next, we investigated the activation of the AMPK-Beclin1 signaling in the epididymal fat of aged mice. Western blotting showed that p-AMPK, p-Beclin1, and p-ULK1 levels in the epididymal fat of aged mice were higher than those of young mice (Fig. 5D and E). Finally, atRA is synthesized from all-*trans* retinal by the ALDH1A family [25], we examined ALDH1A family expression in the epididymal fat of aged mice. The ALDH1A1 protein expression, but not ALDH1A2, increased in the epididymal fat of aged mice compared with young mice (Fig. 5F and G). In other words, the increase of atRA synthetic enzymes may imply high atRA levels in adipose tissues of aged mice.

4. Discussion

In the present study, we showed that atRA induces lipophagy through the AMPK-Beclin1 signaling pathway in mice adipocytes.

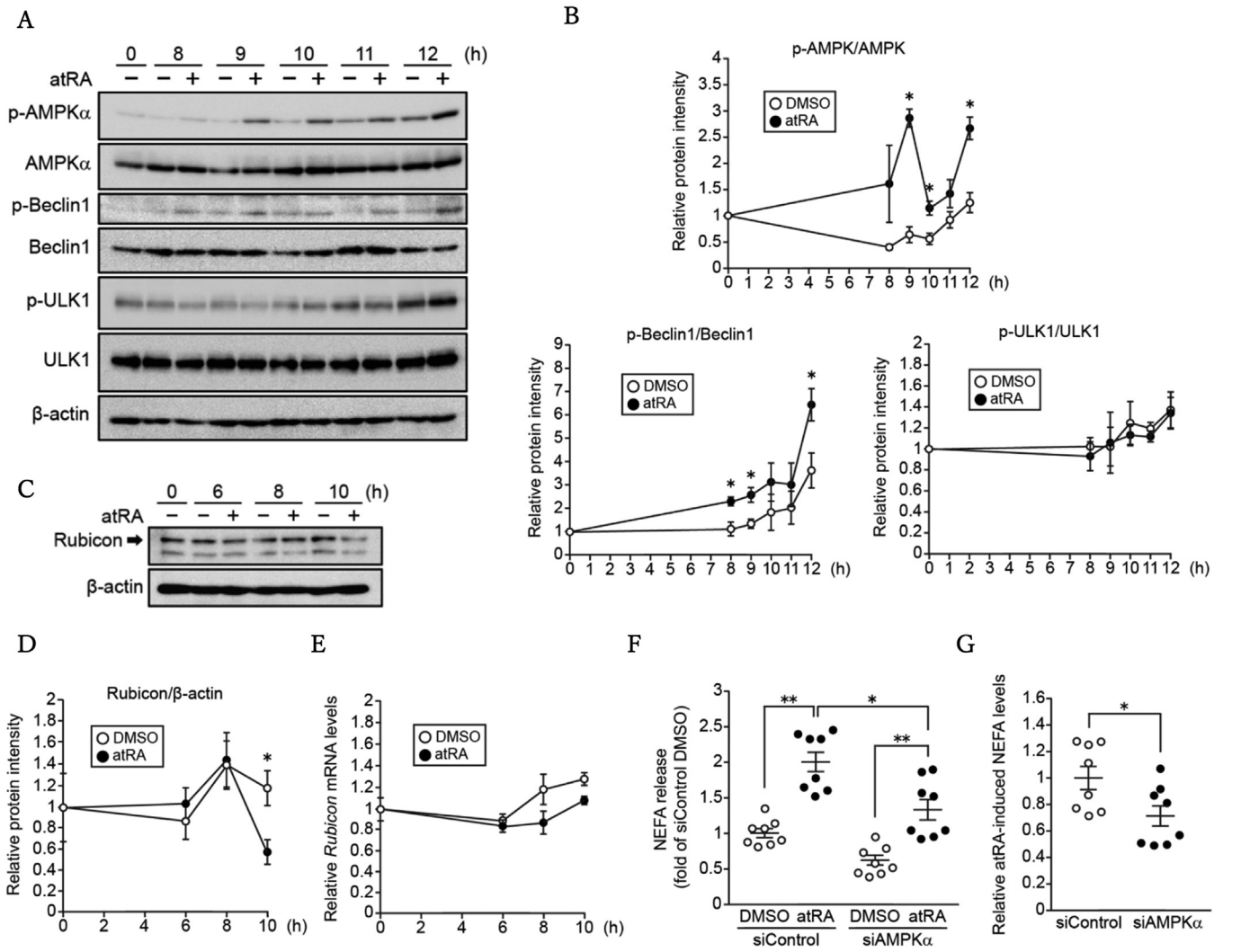

Fig. 3. Effect of atRA on the AMPK-Beclin1 signaling pathway and Rubicon expression in 3T3-L1 adipocytes. (A–D) Western blotting of phosphorylated-AMPKα (p-AMPKα), total AMPKα, phosphorylated-ULK1 (p-ULK1), total ULK1, phosphorylated-Beclin1 (p-Beclin1), total Beclin1, and Rubicon in 3T3-L1 adipocytes treated with 100 nM atRA or 0.1% DMSO (Control) for the indicated periods (n=3–4). β-actin was used as an internal control. (E) The *Rubicon* mRNA levels in 3T3-L1 adipocytes treated with atRA or DMSO (Control) for the indicated periods (0, 6, 8, and 10 h) were detected by real-time PCR (n=3–4). *β-actin* was used as an internal control. $^{*}P<.05$ vs. DMSO (two-tailed unpaired Student's t test). (F, G) 3T3-L1 adipocytes were treated with 100 nM atRA or 0.1% DMSO (Control) in DMEM containing 2% BSA-FFA for 24 h after transfection with 100 pmol *AMPKα1/2* siRNA (siAMPKα) or siControl (n=8). The culture medium was collected and assayed for NEFA content (mEq/L/mg protein). $^{*}P<.05$, $^{**}P<.01$ (one-way ANOVA with a Student-Newman *post-hoc* test). (G) The comparison of atRA-induced NEFA levels (mEq/L/mg protein) in the medium of 3T3-L1 adipocytes treated with siAMPKα or siControl. $^{*}P<.05$ (two-tailed unpaired Student's t test).

We also determined that atRA decreases Rubicon protein in adipocytes and the epididymal fat. Recently, it has been reported that lipophagy contributes to lipolysis in adipocytes [7,35]. These studies have shown the effects of drugs or dietary functional food factors on lipophagy, but it remains unclear whether essential nutrients induce lipophagy in adipocytes. atRA is closely related to lipid metabolism, such as induction of lipolysis through the increase in HSL, inhibition of fat synthesis, and increase in thermogenesis and β-oxidation [8,36]. However, it was not clear whether atRA causes lipophagy. Our study found that each *Atg5*- or *AMPKα1/2*-knockdown partially inhibited the atRA-induced release of NEFA from LDs in mature 3T3-L1 adipocytes. Largely, there are two pathways in which the activation of AMPKα leads to upregulating autophagic flux, such as *via* ULK1 and Beclin1 [16–18]. We confirmed that atRA increased p-AMPKα and p-Beclin1 levels but not p-ULK1 in mature 3T3-L1 adipocytes. The main sensor of cellular energy status in effective all eukaryotic cells is the AMPKα, which is highly conserved across all eukaryotic species. Generally, AMPKα is activated in response to energy stress by sensing increases in AMP/ATP and ADP/ATP ratios [37]. In addition, atRA reduces *Glut1* mRNA expression and contributes to a decrease in intracellular ATP, leading to the activation of AMPK [38]. However, our study showed that atRA slightly increased *Glut1* mRNA expression in differentiated 3T3-L1 cells (Supplementary Fig. S1B). Merhi et al. reported that atRA promoted calcium entry through store-operated calcium channels in APL cells, leading to AMPKα phosphorylation and autophagy [30]. Taken together, atRA may increase p-AMPKα through calcium entry in mouse adipocytes, leading to an increase in p-Beclin1 levels and induction of autophagy.

In the present study, we showed that atRA treatment increases the release of NEFA from LDs in differentiated 3T3-L1 cells, however, atRA administration to mice for 4 weeks did not affect plasma NEFA levels compared with the control group. It has been reported that atRA treatment activates fatty acid oxidation (FAO) in skeletal muscle *via* increasing the expression of genes related to FAO and

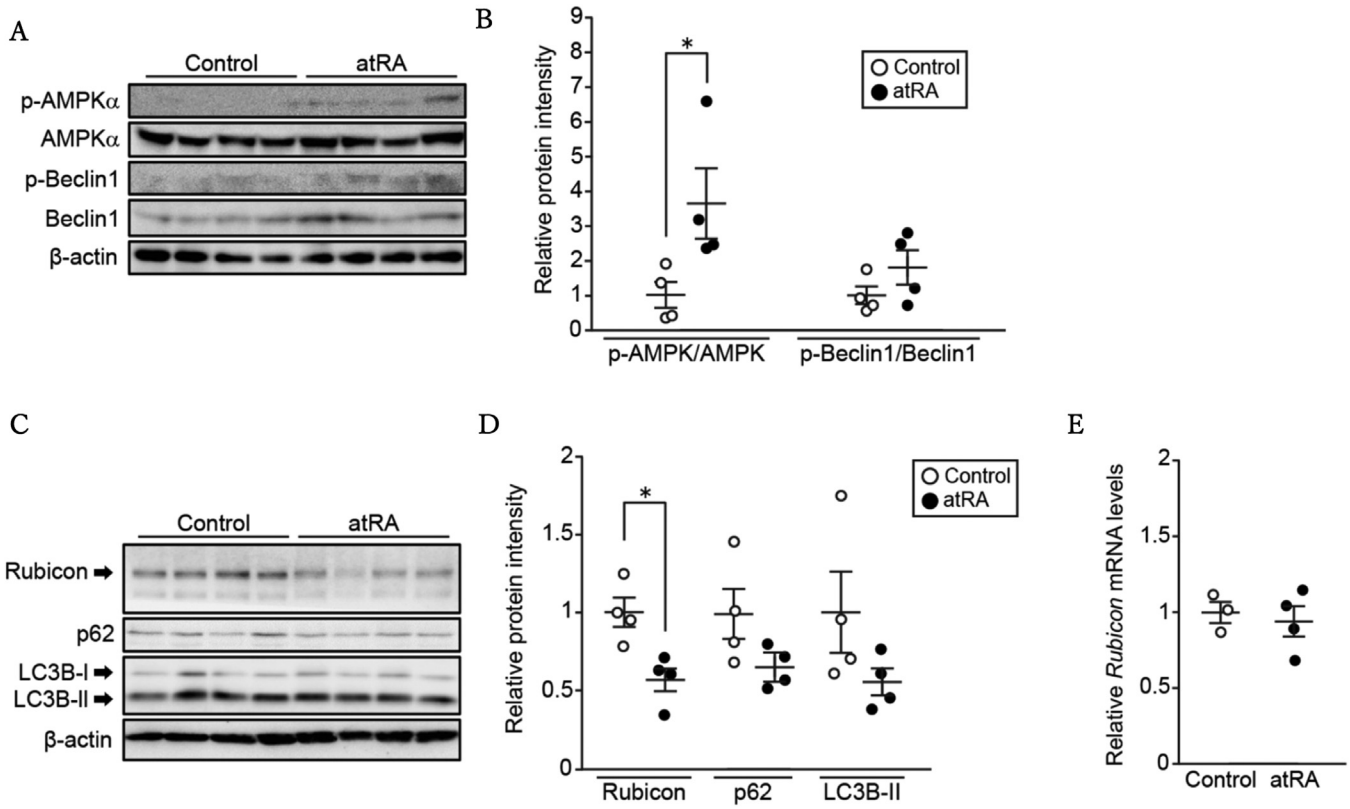

Fig. 4. Effect of atRA on the AMPK-Beclin1 signaling pathway and Rubicon expression in the epididymal fat of mice. Eight-week-old male C57BL/6J mice were treated with 0.1% DMSO (Control) or atRA (10 mg/kg) for 24 h. (A–D) Western blotting of p-AMPKα, total AMPKα, p-Beclin1, total Beclin1, Rubicon, p62, and LC3B in the epididymal fat of mice. (E) The *Rubicon* mRNA in the epididymal fat of mice was detected by real-time PCR. *β-actin* was used as an internal control. Values are mean±S.E.M. (n=3–4). $^{*}P<.05$ (two-tailed unpaired Student's t test).

CD36, fatty acid transporter, in mice [39]. Therefore, the NEFA released from adipocytes by atRA may be used for FAO in skeletal muscle. In addition, we showed that atRA treatment tended to increase plasma TG levels in mice. One of the mechanisms regulating plasma TG levels is lipolysis by lipoprotein lipase (LPL) on the vessel wall [40]. Apo C-III, one of the lipoproteins, suppresses lipolysis by LPL and contributes to high plasma TG levels [41]. Interestingly, it has been reported that atRA increases serum TG levels in rats [42] and apo C-III in human hepatocytes which are the primary cells producing apo C-III [43]. Therefore, atRA might tend to increase plasma TG levels by inhibiting LPL-induced lipolysis through an increase in apo C-III, independent of lipophagy in adipose tissue. For these reasons, the effects of atRA on the NEFA and TG levels might differ between *in vivo* and *in vitro*.

Unlike the AMPK-Beclin1 pathway, Rubicon is known as an autophagy repressor [19]. The present study found that atRA decreased Rubicon protein, not mRNA expression, in 3T3-L1 adipocytes and the epididymal fat. This result suggests that atRA reduces Rubicon protein expression *via* post-transcriptional regulation. Tanaka et al. have shown that palmitic acid increases Rubicon protein expression by inhibiting proteasome-mediated degradation in hepatocytes [44]. Intracellular saturated fatty acids (SFAs: palmitic acid and stearic acid) and monounsaturated fatty acids (MUFAs: palmitoleate and oleate) balance is appropriately controlled by a lipogenic enzyme stearoyl-CoA desaturase (SCD) which catalyzes the conversion of SFAs to MUFAs [45]. That is to say, an increase in SCD expression indicates a decrease in intracellular SFAs. One group reported that atRA upregulated *Scd* mRNA expression in retinal pigment epithelial cells through RAR and RXR [46]. However, we confirmed that atRA did not increase SCD1 protein expression in differentiated 3T3-L1 cells (Supplementary Fig. S2A). Beyond that, high glucose treatment increased Rubicon protein expression *via* phosphorylation of EGFR in podocytes [47]. RAR-selective ligands, including atRA, reduced EGFR levels and the magnitude and duration of EGFR activation in EGF-stimulated cells [48]. However, atRA did not decrease the phosphorylation of EGFR in differentiated 3T3-L1 cells (Supplementary Fig. S2B). These results suggest that atRA decreases Rubicon *via* pathways other than SCD and EGFR in adipocytes. Interestingly, the Rubicon protein was degraded by autophagy in 3T3-L1 adipocytes, just like LC3 and p62 proteins [49]. Therefore, atRA may decrease Rubicon protein through autophagy-mediated degradation of Rubicon in 3T3-L1 adipocytes.

Adiponectin is a secreted cytokine from adipocytes that regulates other metabolic organ functions through some secreted cytokines [50]. Interestingly, adiponectin increases lipolysis by activating lipophagy in breast cancer cells [51]. Although Kosacka et al. have reported that up-regulated autophagy inhibits adiponectin expression in visceral adipocytes of rats [52], it is unclear whether lipophagy affects adiponectin expression. Unfortunately, there are currently no lipophagy selective inducers. Because we confirmed that Torin 1, an autophagy inducer, increased the release of NEFA levels from LDs in differentiated 3T3-L1 cells in this study, we considered Torin 1 a lipophagy inducer. Then, we found that adiponectin protein expression decreased after 8, 12, and 20 h of Torin 1 treatment (Supplementary Fig. S3A). Based on this finding, lipophagy may decrease adiponectin in mouse adipocytes. In addition, although it has been reported that the reduction of Rubicon suppresses adiponectin expression [21], the effect of adiponectin on Rubicon has not been investigated. Our study showed that

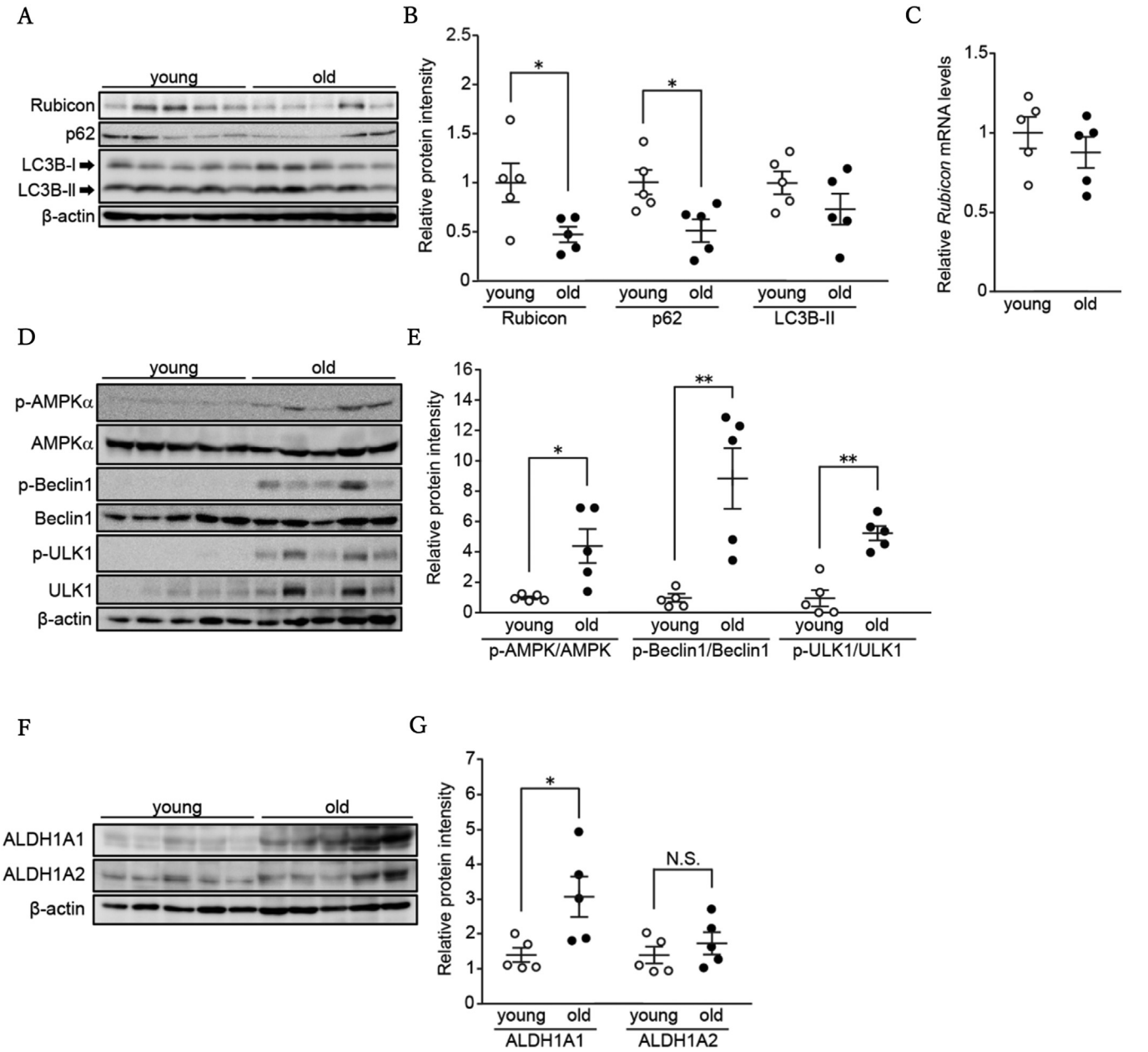

Fig. 5. The expression of Rubicon and ALDH1As in the epididymal fat of mice. The epididymal fat samples were from 8-week-old and 100-week-old male C57BL/6J mice. (A, B, D–G) Western blotting of Rubicon, p62, LC3B, p-AMPKα, total AMPKα, p-Beclin1, total Beclin1, p-ULK1, total ULK1, ALDH1A1, and ALDH1A2 in the epididymal fat. β-actin was used as an internal control. (C) The *Rubicon* mRNA was detected by real-time PCR in the epididymal fat. Values are mean±S.E.M. (n=5). $^{*}P<.05$, $^{**}P<.01$ (two-tailed unpaired Student's t test). NS, not significant.

atRA decreases Rubicon expression at 10 h in differentiated 3T3-L1 cells. Interestingly, high-vitamin A diets dramatically decline adiponectin expression in the WAT of mice [53]. In addition, we confirmed that atRA did not change adiponectin expression at 6, 8, 10 h in differentiated 3T3-L1 cells before atRA decreased Rubicon expression (Supplementary Fig. S3B). Although these results suggest that adiponectin may not affect Rubicon expression in mouse adipocytes, further study is necessary to understand the interplay between adiponectin and Rubicon, as well as the regulatory mechanisms influencing Rubicon, especially in response to adiponectin and atRA.

RAS signaling is essential in driving normal physiological cellular proliferation, and dysregulation of this signaling pathway commonly occurs during tumorigenesis [54]. Failure of autophagy is associated with cancer in breast, ovarian, colon, lung, and brain [55]. Interestingly, Sabarwal et al. reported that the expression of Rubicon is minimal in normal renal epithelial cells (RPTEC), whereas it is significantly overexpressed in human renal cancer cell lines (786-0, ACHN, and Caki-1) [56]. That is to say, these reports suggest that Rubicon may be involved in the regulation of not only autophagy but also the RAS pathway and cancer growth/progression. Hepatocarcinogenesis is closely related to the impaired metabolism of retinoids. The vitamin A content of hepatoma tissue starts to decline early in carcinogenesis [57]. A cohort study demonstrated an inverse dose-response relation between the serum retinol level before diagnosis and the development of hepatoma [58]. In addi-

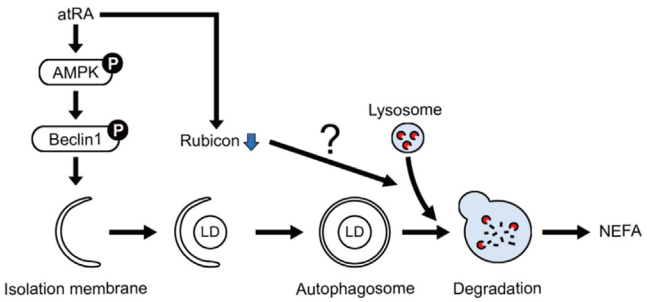

Fig. 6. Schematic illustration of atRA-induced lipophagy through activating the AMPK-Beclin1 signaling pathway in adipocytes. The atRA-induced activation of the AMPK-Beclin1 signaling pathway causes lipophagy, resulting in the NEFA release from LDs. atRA also decreases Rubicon expression in adipocytes, which may be associated with lipophagy.

tion, clinical trials have shown that acyclic retinoids have an inhibitory effect on hepatocarcinogenesis. After 1 year of treatment with acyclic retinoids, patients who had undergone liver cancer treatment were found to have a reduced incidence of liver cancer recurrence for approximately 4 years after the end of treatment [59]. In the present study, we showed that atRA reduced Rubicon expression, and if the mechanism can be elucidated, it may be a potential target for cancer therapy research.

Although Rubicon protein decreases in the adipose tissue of aged mice, the underlying molecular mechanism remains unclear [21]. The epidemiological study reported that the serum concentration of retinol increased with aging [60]. All-*trans* retinol is first converted to all-*trans* retinal and then irreversibly oxidized by the ALDH1A family to form atRA [25]. ALDH1A1 is the most highly expressed member of the ALDH1A family in adipocytes [61]. In the present study, we confirmed the increase of ALDH1A1 protein expression and the phosphorylation of AMPK and Beclin1 but the decrease of Rubicon protein expression in the epididymal fat of aged mice compared to young mice. In addition, *Aldh1a1* knockdown decreased the phosphorylation of AMPK and Beclin1 and increased Rubicon protein expression in differentiated 3T3-L1 cells (Supplementary Fig. S4A and B). Therefore, these results suggest that atRA levels are higher in the adipose tissue of aged mice than in young mice, resulting in increased atRA, which may partially contribute to inducing autophagy by activating the AMPK-Beclin1 signaling pathway and reducing Rubicon in adipocytes of aged mice (Supplementary Fig. S4C). ALDH1A1 expression is induced by transcriptional regulation *via* CCAAT/enhancer-binding protein β (C/EBPβ) and β-catenin [62]. It has also been reported that protein expression of C/EBPβ increases in the brane of aged mice, and β-catenin increases in the skin of aged mice [63,64]. Therefore, C/EBPβ and β-catenin may upregulate ALDH1A1 expression, increasing atRA levels in the epididymal fat of aged mice. Based on these reports, we confirmed whether aged mice showed an increase in *Aldh1a1* mRNA expression in the adipose tissue; however, aging did not increase them (Supplementary Fig. S5). Further studies will be required to identify the mechanisms by which aging induces an increase in ALDH1A1 protein levels.

In conclusion, as shown in Figure 6, the present study showed that atRA induces lipophagy by activating the AMPK-Beclin1 signaling pathway in adipocytes. atRA also decreases Rubicon expression in adipocytes. In addition, atRA can decrease Rubicon protein in adipocytes and the epididymal fat, which may contribute to decreasing Rubicon expression in the epididymal fat of aged mice with increased ALDH1A1 expression. To our knowledge, this is the first study to find a nutrient factor that induces lipophagy and decreases Rubicon in adipocytes.

Funding

This work was supported by JSPS KAKENHI Grant Numbers JP20K21761, JP21H03359 (to M. Masuda), JP19H04053, JP23H03329 (to Y. Taketani), Otsuka Pharmaceutical (to M. Masuda), and JST, the establishment of university fellowships towards the creation of science technology innovation, Grant Number JPMJFS2130 (to Y. Mori). This work was also supported by Research Clusters of Tokushima University: Research Cluster for Precision Nutrition (to Y. Taketani).

Declaration of competing interest

The authors declare that they have no conflicts of interest with the contents of this article.

CRediT authorship contribution statement

Yuki Mori: Methodology, Formal analysis, Investigation, Writing – original draft. **Masashi Masuda:** Conceptualization, Validation, Writing – review & editing, Supervision, Project administration, Funding acquisition. **Risa Yoshida-Shimizu:** Methodology, Formal analysis, Investigation. **Saki Aoyagi:** Formal analysis. **Yuichiro Adachi:** Investigation. **Anh The Nguyen:** Data curation. **Yusuke Maruyama:** Visualization. **Yosuke Okumura:** Validation. **Yuki Kamei:** Visualization. **Maiko Sakai:** Formal analysis. **Kohta Ohnishi:** Conceptualization, Resources, Validation. **Hirokazu Ohminami:** Visualization. **Yutaka Taketani:** Writing – review & editing, Supervision, Project administration, Funding acquisition.

Acknowledgments

We thank Dr. N. Mizushima (The University of Tokyo) for providing pMRX-IP-GFP-LC3-RFP-LC3ΔG plasmid for technical assistance. We also thank Fujii Memorial Institute of Medical Science, Support Center for Advanced Medical Sciences, TokushimaUniversity Graduate School of Biomedical Sciences, A. Yamazaki-Uebanso, M. Ipponmatsu, S. Li, R. Kimura, K. Sasaki, Y. Nobe, N. Yamamoto, and Y. Tsuda (Department of Clinical Nutrition and Food Management, Institute of Biomedical Sciences, Tokushima University Graduate School) for technical assistance.

Supplementary materials

Supplementary material associated with this article can be found, in the online version, at doi:10.1016/j.jnutbio.2024.109589.

References

[1] Blüher M. Obesity: global epidemiology and pathogenesis. Nat Rev Endocrinol 2019;15:288–98.
[2] Heymsfield SB, Wadden TA. Mechanisms, pathophysiology, and management of obesity. N Engl J Med 2017;376:254–66.
[3] Kopelman PG. Obesity as a medical problem. Nature 2000;404:635–43.
[4] Bray GA. A concise review on the therapeutics of obesity. Nutrition 2000;16:953–60.
[5] Abuduli M, Ohminami H, Otani T, Kubo H, Ueda H, Kawai Y, et al. Effects of dietary phosphate on glucose and lipid metabolism. Am J Physiol Endocrinol Metab 2016;310:E526–38.
[6] Imi Y, Yabiki N, Abuduli M, Masuda M, Yamanaka-Okumura H, Taketani Y. High phosphate diet suppresses lipogenesis in white adipose tissue. J Clin Biochem Nutr 2018;63:181–91.
[7] Masuda M, Yoshida-Shimizu R, Mori Y, Ohnishi K, Adachi Y, Sakai M, et al. Sulforaphane induces lipophagy through the activation of AMPK-mTOR-ULK1 pathway signaling in adipocytes. J Nutr Biochem 2022;106:109017.
[8] Berry DC, Noy N. All-trans-retinoic acid represses obesity and insulin resistance by activating both peroxisome proliferation-activated receptor beta/delta and retinoic acid receptor. Mol Cell Biol 2009;29:3286–96.

[9] Zechner R, Kienesberger PC, Haemmerle G, Zimmermann R, Lass A. Adipose triglyceride lipase and the lipolytic catabolism of cellular fat stores. J Lipid Res 2009;50:3–21.
[10] Duncan RE, Ahmadian M, Jaworski K, Sarkadi-Nagy E, Sul HS. Regulation of lipolysis in adipocytes. Annu Rev Nutr 2007;27:79–101.
[11] Singh R, Kaushik S, Wang Y, Xiang Y, Novak I, Komatsu M, et al. Autophagy regulates lipid metabolism. Nature 2009;458:1131–5.
[12] Mizushima N, Yoshimori T, Ohsumi Y. The role of Atg proteins in autophagosome formation. Annu Rev Cell Dev Biol 2011;27:107–32.
[13] Shibutani ST, Yoshimori T. A current perspective of autophagosome biogenesis. Cell Res 2014;24:58–68.
[14] Mizushima N, Komatsu M. Autophagy: renovation of cells and tissues. Cell 2011;147:728–41.
[15] Makino S, Kawamata T, Iwasaki S, Ohsumi Y. Selectivity of mRNA degradation by autophagy in yeast. Nat Commun 2021;12:2316.
[16] Kim J, Kundu M, Viollet B, Guan KL. AMPK and mTOR regulate autophagy through direct phosphorylation of Ulk1. Nat Cell Biol 2011;13:132–41.
[17] Roach PJ. AMPK ->ULK1 ->autophagy. Mol Cell Biol 2011;31:3082–3084.
[18] Kim J, Kim YC, Fang C, Russell RC, Kim JH, Fan W, et al. Differential regulation of distinct Vps34 complexes by AMPK in nutrient stress and autophagy. Cell 2013;152:290–303.
[19] Matsunaga K, Saitoh T, Tabata K, Omori H, Satoh T, Kurotori N, et al. Two Beclin 1-binding proteins, Atg14L and Rubicon, reciprocally regulate autophagy at different stages. Nat Cell Biol 2009;11:385–96.
[20] Nakamura S, Oba M, Suzuki M, Takahashi A, Yamamuro T, Fujiwara M, et al. Suppression of autophagic activity by Rubicon is a signature of aging. Nat Commun 2019;10:847.
[21] Yamamuro T, Kawabata T, Fukuhara A, Saita S, Nakamura S, Takeshita H, et al. Age-dependent loss of adipose Rubicon promotes metabolic disorders via excess autophagy. Nat Cell Commun 2020;11:4150.
[22] Clagett-Dame M, DeLuca HF. The role of vitamin A in mammalian reproduction and embryonic development. Annu Rev Nutr 2002;22:347–81.
[23] Hall JA, Grainger JR, Spencer SP, Belkaid Y. The role of retinoic acid in tolerance and immunity. Immunity 2011;35:13–22.
[24] Rhinn M, Dollé P. Retinoic acid signalling during development. Development 2012;139:843–58.
[25] Xi J, Yang Z. Expression of RALDHs (ALDH1As) and CYP26s in human tissues and during the neural differentiation of P19 embryonal carcinoma stem cell. Gene Expr Patterns 2008;8:438–42.
[26] Botella-Carretero JI, Balsa JA, Vázquez C, Peromingo R, Díaz-Enriquez M, Escobar-Morreale HF. Retinol and alpha-tocopherol in morbid obesity and nonalcoholic fatty liver disease. Obes Surg 2010;20:69–76.
[27] Liu Y, Chen H, Mu D, Fan J, Song J, Zhong Y, et al. Circulating retinoic acid levels and the development of metabolic syndrome. J Clin Endocrinol Metab 2016;101:1686–92.
[28] Chambon P. A decade of molecular biology of retinoic acid receptors. FASEB J 1996;10:940–54.
[29] Schug TT, Berry DC, Shaw NS, Travis SN, Noy N. Dual transcriptional activities underlie opposing effects of retinoic acid on cell survival. Cell 2007;129:723–33.
[30] Merhi F, Alvarez-Valadez K, Trepiana J, Lescoat C, Groppi A, Dupuy JW, et al. Targeting CAMKK2 and SOC channels as a novel therapeutic approach for sensitizing acute promyelocytic leukemia cells to all-trans retinoic acid. Cells 2021;10:3364.
[31] Kaizuka T, Morishita H, Hama Y, Tsukamoto S, Matsui T, Toyota Y, et al. An autophagic flux probe that releases an internal control. Mol Cell 2016;64:835–49.
[32] Pu M, Zheng W, Zhang H, Wan W, Peng C, Chen X, et al. ORP8 acts as a lipophagy receptor to mediate lipid droplet turnover. Protein Cell 2023;14:653–67.
[33] Brasaemle DL, Subramanian V, Garcia A, Marcinkiewicz A, Rothenberg A. Perilipin A and the control of triacylglycerol metabolism. Mol Cell Biochem 2009;326:15–21.
[34] Sztalryd C, Brasaemle DL. The perilipin family of lipid droplet proteins: gatekeepers of intracellular lipolysis. Biochim Biophys Acta Mol Cell Biol Lipids 2017;1862:1221–32.
[35] Zhang X, Wu D, Wang C, Luo Y, Ding X, Yang X, et al. Sustained activation of autophagy suppresses adipocyte maturation via a lipolysis-dependent mechanism. Autophagy 2020;16:1668–82.
[36] Bonet ML, Ribot J, Palou A. Lipid metabolism in mammalian tissues and its control by retinoic acid. Biochim Biophys Acta 2012;1821:177–89.
[37] Garcia D, Shaw RJ. AMPK: mechanisms of cellular energy sensing and restoration of metabolic balance. Mol Cell 2017;66:789–800.
[38] Ishijima N, Kanki K, Shimizu H, Shiota G. Activation of AMP-activated protein kinase by retinoic acid sensitizes hepatocellular carcinoma cells to apoptosis induced by sorafenib. Cancer Sci 2015;106:567–75.
[39] Amengual J, García-Carrizo FJ, Arreguín A, Mušinović H, Granados N, Palou A, et al. Retinoic acid increases fatty acid oxidation and irisin expression in skeletal muscle cells and impacts irisin in vivo. Cell Physiol Biochem 2018;46:187–202.
[40] Paragh G, Németh Á, Harangi M, Banach M, Fülöp P. Causes, clinical findings and therapeutic options in chylomicronemia syndrome, a special form of hypertriglyceridemia. Lipids Health Dis 2022;21:21.
[41] Maeda N, Li H, Lee D, Oliver P, Quarfordt SH, Osada J. Targeted disruption of the apolipoprotein C-III gene in mice results in hypotriglyceridemia and protection from postprandial hypertriglyceridemia. J Biol Chem 1994;269:23610–16.
[42] Standeven AM, Beard RL, Johnson AT, Boehm MF, Escobar M, Heyman RA, et al. Retinoid-induced hypertriglyceridemia in rats is mediated by retinoic acid receptors. Fundam Appl Toxicol 1996;33:264–71.
[43] Vu-Dac N, Gervois P, Torra IP, Fruchart JC, Kosykh V, Kooistra T, et al. Retinoids increase human apo C-III expression at the transcriptional level via the retinoid X receptor. Contribution to the hypertriglyceridemic action of retinoids. J Clin Invest 1998;102:625–32.
[44] Tanaka S, Hikita H, Tatsumi T, Sakamori R, Nozaki Y, Sakane S, et al. Rubicon inhibits autophagy and accelerates hepatocyte apoptosis and lipid accumulation in nonalcoholic fatty liver disease in mice. Hepatology 2016;64:1994–2014.
[45] Miyazaki M, Ntambi JM. Role of stearoyl-coenzyme A desaturase in lipid metabolism. Prostaglandins Leukot Essent Fat Acids 2003;68:113–21.
[46] Samuel W, Kutty RK, Nagineni S, Gordon JS, Prouty SM, Chandraratna RA, et al. Regulation of stearoyl coenzyme A desaturase expression in human retinal pigment epithelial cells by retinoic acid. J Biol Chem 2001;276:44–50.
[47] Li Y, Pan Y, Cao S, Sasaki K, Wang Y, Niu A, et al. Podocyte EGFR inhibits autophagy through upregulation of Rubicon in type 2 diabetic nephropathy. Diabetes 2021;70:562–76.
[48] Sah JF, Eckert RL, Chandraratna RA, Rorke EA. Retinoids suppress epidermal growth factor-associated cell proliferation by inhibiting epidermal growth factor receptor-dependent ERK1/2 activation. J Biol Chem 2002;277:28–35.
[49] Yamamuro T, Nakamura S, Yanagawa K, Tokumura A, Kawabata T, Fukuhara A, et al. Loss of RUBCN/rubicon in adipocytes mediates the upregulation of autophagy to promote the fasting response. Autophagy 2022;18:2686–96.
[50] Achari AE, Jain SK. Adiponectin, a therapeutic target for obesity, diabetes, and endothelial dysfunction. Int J Mol Sci 2017;18:1321.
[51] Pham DV, Park PH. Adiponectin triggers breast cancer cell death via fatty acid metabolic reprogramming. J Exp Clin Cancer Res 2022;41:9.
[52] Kosacka J, Nowicki M, Paeschke S, Baum P, Blüher M, Klöting N, et al. Up-regulated autophagy: as a protective factor in adipose tissue of WOKW rats with metabolic syndrome. Diabetol Metab Syndr 2018;10:13.
[53] Landrier JF, Kasiri E, Karkeni E, Mihaly J, Beke G, Weiss K, et al. Reduced adiponectin expression after high-fat diet is associated with selective up-regulation of ALDH1A1 and further retinoic acid receptor signaling in adipose tissue. FASEB J 2017;31:203–11.
[54] Cargnello M, Roux PP. Activation and function of the MAPK and their substrates, the MAPK-activated protein kinases. Microbiol Mol Biol Rev 2011;75:50–83.
[55] Levine B, Kroemer G. Biological functions of autophagy genes: a disease perspective. Cell 2019;176:11–42.
[56] Sabarwal A, Wedel J, Liu K, Zurakowski D, Chakraborty S, Flynn E, et al. A Combination therapy using an mTOR inhibitor and Honokiol effectively induces autophagy through the modulation of AXL and Rubicon in renal cancer cells and restricts tumor growth following organ transplantation. Carcinogenesis 2022;43:360–70.
[57] Muto Y, Omori M. A novel cellular retinoid-binding protein, F-type, in hepatocellular carcinoma. Ann N Y Acad Sci 1981;359:91–103.
[58] Yu MW, Hsieh HH, Pan WH, Yang CS, Chen CJ. Vegetable consumption, serum retinol level, and risk of hepatocellular carcinoma. Cancer Res 1995;55:1301–5.
[59] Muto Y, Moriwaki H, Ninomiya M, Adachi S, Saito A, Takasaki S, et al. Prevention of second primary tumors by an acylic retinoid, polyprenoic acid, in patients with hepatocellular carcinoma. Hepatoma Prevention Study Group. N Engl J Med 1996;334:1561–7.
[60] Gueguen S, Leroy P, Gueguen R, Siest G, Visvikis S, Herbeth B. Genetic and environmental contributions to serum retinol and alpha-tocopherol concentrations: the Stanislas Family Study. Am J Clin Nutr 2005;81:1034–44.
[61] Reichert B, Yasmeen R, Jeyakumar SM, Yang F, Thomou T, Alder H, et al. Concerted action of aldehyde dehydrogenases influences depot-specific fat formation. Mol Endocrinol 2011;25:799–809.
[62] Poturnajova M, Kozovska Z, Matuskova M. Aldehyde dehydrogenase 1A1 and 1A3 isoforms: mechanism of activation and regulation in cancer. Cell Signal 2021;87:110120.
[63] Wang ZH, Gong K, Liu X, Zhang Z, Sun X, Wei ZZ, et al. C/EBPβ regulates delta-secretase expression and mediates pathogenesis in mouse models of Alzheimer's disease. Nat Commun 2018;9:1784.
[64] Zhang Z, Lei M, Xin H, Hu C, Yang T, Xing Y, et al. Wnt/β-catenin signaling promotes aging-associated hair graying in mice. Oncotarget 2017;8:69316–27.